1   Impact of winter roads on boreal peatland carbon exchange

2

3   Maria Strack[1*], Divya Softa[1], Melanie Bird[2], and Bin Xu[2]

4   1. Department of Geography and Environmental Management, University of Waterloo,

5   Waterloo, ON

6   2. NAIT Boreal Research Institute, Peace River, AB

7   *corresponding author

8   200 University Ave W

9   Waterloo, ON, CANADA N2L 3G1

10   mstrack@uwaterloo.ca

11   phone: +1 519 888-4567 x30164

12

13   Running head: Peatland carbon exchange on winter roads

16

17

Abstract

Across Canada's boreal forest, linear disturbances, including cutlines such as seismic lines and roads, crisscross the landscape to facilitate resource exploration and extraction; many of these linear disturbances cross peatland ecosystems. Changes in tree canopy cover and the compression of the peat by heavy equipment alters local thermal, hydrological and ecological conditions, likely changing carbon exchange on the disturbance, and possibly in the adjacent peatland. We measured bulk density, water table, soil temperature, plant cover, and CO_2 and CH_4 flux along triplicate transects crossing a winter road through a wooded fen near Peace River, Alberta, Canada. Sample plots were located 1, 5 and 10 m from the road on both sides with an additional three plots on the road. Productivity of the overstory trees, when present, was also determined. The winter road had higher bulk density, shallower water table, higher graminoid cover, and thawed earlier than the adjacent peatland. Tree productivity and CO_2 flux varied between the plots, and there was no clear pattern in relation to distance from the road. The plots on the winter road acted as a greater CO_2 sink and greater CH_4 source compared to the adjacent peatland. with plots on the winter road emitting on average (standard error) 479 (138) compared to 41 (10) mg CH_4 m^{-2} d^{-1} in the adjacent peatland. Considering both gases, global warming potential increased from 70 to 250 g CO_2e m^{-2} yr^{-1} in the undisturbed area to 2100 g CO_2e m^{-2} yr^{-1} on the winter road. Although carbon fluxes on any given cutline through peatland will vary depending on level of compaction, line width and vegetation community shifts, the large number of linear disturbances in Canada's boreal forest and slow recovery on peatland ecosites suggest they could represent an important source anthropogenic greenhouse gas source.

Introduction

In Canada's boreal zone, particularly in the province of Alberta, resource extraction, including oil sands exploitation and forestry, has resulted in a grid of exploration lines (often referred to as seismic lines), access roads and well pads. Timoney and Lee (2001) estimated that $1 - 2$ million km of seismic lines existed in the province; the number is likely higher today given continued oil sands extraction. Based on approved in-situ oil and gas extraction leases in Alberta in 2005 it was estimated that at least 30 000 km of access roads would be constructed in Alberta's boreal forest if all leases were developed (Schneider & Dyer, 2006), and it has been estimated that linear disturbances account for 80% of boreal anthropogenic disturbance (Pasher *et al*., 2013). Given the large proportion of peatland in this region, many of these disturbance features exist on peatland areas; however, their impact on carbon dioxide (CO_2) and methane (CH_4) exchange is poorly understood. As northern peatlands play an important role in the global carbon (C) cycle as long term sinks for atmospheric CO_2 (e.g. Frolking & Roulet, 2007), stores of soil organic matter (Loisel *et al*., 2014) and sources of CH_4 (Bridgham *et al*., 2013) it is important to understand how disturbances alter C exchanges in these ecosystems. Moreover, quantifying the impact of linear disturbances on peatland C exchange will help improve estimates of wetland greenhouse gas (GHG) emissions related to land-use in Canada (IPCC, 2014). This study investigated the impact of a winter road on growing season CO_2 and CH_4 exchange both on the winter road and in the adjacent peatland in a wooded fen near Peace River, AB.

Although research has been published on vegetation change and thermal effects related to linear disturbance (e.g., Braverman & Quinton, 2016; van Rensen *et al*., 2015), very little data is available on peatland C exchange related to the impact of linear disturbance. Unlike semi-permanent and permanent access roads built with padded mineral material to allow year-round

63 access by equipment, construction of temporary and exploratory linear features such as winter

64 roads and seismic lines involves the flattening and removal of trees, shrubs, and herbs at the base

65 without significant disturbance to the ground layer of mosses. Construction and exploration usually

66 occur in frozen winter conditions but repeated access is also common under soft ground conditions.

67 Vegetation recovery from remaining roots and rhizomes is possible (e.g., van Rensen *et al*., 2015)

68 but often compromised by changes in chemical and hydrological conditions caused by repeated use

69 and continued compaction of surface.

70   Removal of trees from the footprint of the winter road or cutline itself will remove the

71 canopy biomass and tree net primary productivity (NPP), potentially reducing C uptake by the

72 ecosystem unless the understory productivity increases to compensate for the loss. Vitt *et al*. (2000)

73 report aboveground biomass of non-permafrost treed continental peatlands at 750 and 775 g m^{-2}

74 for fens and bogs, respectively and Wieder *et al*. (2009) report peak NPP for black spruce stands

75 in Alberta bogs at 131 ± 208 g C m^{-2} yr^{-1}. Campbell *et al.* (2000) collected literature data across

76 North American peatlands and report ranges from treed sites of 351–7300 g m^{-2} for biomass and

77 27–310 g m^{-2} yr^{-1} for NPP; therefore, removal of trees from peatland winter roads and cutlines

78 could reduce C stocks and uptake by these amounts. Moreover, changes to local hydrology on the

79 disturbance also have the potential to alter C exchange. Subsidence of the peat on the winter road

80 results in wetter conditions during the growing season (Williams *et al*., 2013) and thus CH$_4$ flux is

81 expected to be higher on the road than in adjacent peatland areas. Wetter conditions increase peat

82 thermal conductivity (Braverman & Quinton, 2016), while removal of trees from the road will

83 reduce shading, both of which could lead to higher temperatures that would increase the rate of

84 enzymatically driven reactions (e.g., oxidation of organic matter and CH$_4$ production/oxidation).

85 Finally, changes in the plant community in response to hydrologic change will alter litter type with

86 potential for changes in decomposition rate (e.g., Moore *et al.,* 2008) and CH_4 production (e.g.,

87 Strack *et al*., 2017).

88 Compression and subsidence of peat on the winter road could also alter local hydrology and

89 affect the water table in the adjacent peatland. Semi-permanent and permanent roads involving the

90 placement of mineral soil fill have been reported to block the movement of water creating flooding

91 upstream of the road (Gillies, 2011; Patterson & Cooper, 2007). However, since no fill is placed

92 on cutlines, it is unclear if hydrological impacts from altered peat properties on the disturbance will

93 impact the surrounding peatland and if so, whether C fluxes will be affected. If conditions become

94 drier, increased tree growth (e.g., Choi *et al*., 2007; Munir *et al*., 2015), higher rates of soil

95 respiration (e.g., Strack *et al*., 2006; Munir *et al*., 2015) and reduced CH_4 flux are expected (e.g.,

96 Strack *et al*., 2004; Munir & Strack, 2014), while wetting would have opposite effects and could

97 enhance moss productivity (e.g., Weltzin *et al*., 2003).

98 Given the lack of data on C exchange related to peatland cutlines, the objectives of this

99 study were to: 1) determine the growing season peatland understory CO_2 and CH_4 fluxes on the

100 winter road and in the area 1–10 m on either side of the road, 2) evaluate controls (plant cover,

101 water table, temperature) on CO_2 and CH_4 fluxes, 3) determine biomass and annual NPP of the

102 overstory at the same locations, and 4) estimate changes in the C balance and GHG flux on the

103 winter road compared to the adjacent peatland.

104

105 **Methods**

106 *Study site*

107 The study area (56° 23'53.14 N, 116° 53'24.03 W) is located approximately 40 km northeast of

108 Peace River, AB, Canada (Figure 1). A variety of disturbances related to oil sands extraction are

109   present in the study area including seismic lines, winter roads and well pads. The area is boreal

110   forest with a mix of upland forest and peatlands with the majority of peatlands in the immediate

111   area classified as wooded fens (Halsey *et al*., 2003). The studied winter road passes through a

112   wooded fen and is 6-7 m in width, similar to many access paths and conventional 2-D seismic lines

113   built prior to the late 1990s (Lee & Boutin, 2006). As wooded fens account for 37% of peatland

114   cover in western Canada (Vitt *et al*., 2000), this study site is likely representative of many winter

115   roads and seismic lines in this region.

116   We do not have a detailed history of the winter road under study, but satellite images show

117   that it was cleared as a seismic line by ~1999–2000 with use as a winter road likely starting in 2006

118   when the nearby well pad was constructed. Conversion of seismic lines to access paths is common

119   in this region (Lee & Boutin, 2006). Reclamation activities took place on the well pad in late 2011,

120   after which regular traffic on this section of winter road ceased. Some reclamation activities took

121   place on the winter road in March 2014, but the present study was conducted in control areas where

122   vegetation and peat on the winter road had not been altered by these reclamation activities.

123   Campbell and Bergeron (2012) reported significant differences in vegetation community on winter

124   roads compared to adjacent peatland in northern Ontario with no effect of time since abandonment,

125   over seven years, on winter road vegetation. Even decades after construction, there is limited

126   vegetation recovery on 2-D seismic lines through peatlands in Alberta (Lee & Boutin, 2006; van

127   Rensen *et al*., 2015), suggesting that conditions at the study site are likely similar to those present

128   during its use as a winter road.

129   Triplicate plots were located on the winter road and at each of 1 m, 5 m and 10 m on either

130   side of the road in transects (Figure 1). Plots were placed such that microtopography was

131   represented across the triplicate locations and equally represented at each distance from the road

132   (i.e., one high hummock, low hummock and hollow at each distance), but microforms could not be

133   replicated at each sampling location given the effort required for C flux measurements. Plots were

134   installed in late May 2014 once the ground was thawed enough to do so and measurements began

135   the first week of June and continued at least monthly until late September 2014. Measurements

136   were continued May–September, 2015 such that each plot was measured 12–13 times over the two-

137   year period. In August 2014, a tree survey was conducted surrounding each study zone. Trees were

138   measured in plots parallel to the winter road to try to capture any impact of the disturbance. Each

139   plot was 10 m long and 3 m wide and bracketed the C flux sampling plot location (0–3 m, 3–6 m,

140   and 8–11 m from the road on both sides). Due to the high density of trees in the eastern study area,

141   these plots were divided in half so that each was 5 m long and 3 m wide, and this resulted in

142   triplicate tree plots at each distance relative to the winter road.

143

144   *Carbon dioxide flux*

145   Carbon dioxide exchange was determined using the closed chamber method. The net

146   ecosystem exchange of CO_2 in the understory (NEus) was determined with a clear acrylic chamber

147   ($60\times60\times30$ cm) placed on a stainless steel collar (60×60 cm) permanently installed at each

148   sampling plot. A groove in the collar held the chamber and was filled with water to create a seal.

149   A battery-operated fan installed inside the chamber circulated the headspace air throughout the

150   measurement period and the chamber was lifted from the collar between each measurement and

151   allowed to equilibrate to ambient CO_2 concentration and temperature. The concentration of CO_2

152   was determined inside the chamber at 15 to 30-second intervals for a maximum of 2.5 minutes

153   using a portable infrared gas analyzer (EGM-4, PPSystems, Massachusetts, USA). The linear

154   change in CO_2 concentration over time was used to calculate NEus. Ecosystem respiration (ER)

155   was determined by darkening the chamber with an opaque shroud. Gross ecosystem photosynthesis

156   (GEP) was calculated as the difference between NEE and ER. Measurements were made in full

157   sun and under a variety of shades so that light response curves could be constructed. Maximum

158   rate of GEP and NEus (GEP_{max}, $NEus_{max}$ sensu Bubier *et al.*, 2003) was determined at each plot

159   from full sun measurements. We use the sign convention that positive values indicate a release of

160   CO_2 from the ecosystem to the atmosphere.

161

162   *Methane flux*

163   Methane flux was determined with opaque closed chambers ($60 \times 60 \times 30$ cm) equipped with

164   a battery-operated fan to circulate headspace air. Chambers were placed on the collars described

165   above and gas samples were collected 7, 15, 25 and 35 minutes after closure and stored in pre-

166   evacuated vials (Exetainer, Labco Ltd., UK). The concentration of CH_4 in the samples was

167   determined on a Varian 3800 gas chromatograph (Agilent Technologies Canada Inc, Ontario,

168   Canada) equipped with a flame ionization detector. Methane flux was determined from the linear

169   change in concentration over time. In cases where the initial CH_4 concentration was < 5 ppm and

170   the concentration over the closure time changed less than the precision of the GC ($\pm 5\%$), the flux

171   was considered zero. Outside of this exception, if the concentrations did not linearly increase over

172   time ($R^2 < 0.70$), they were removed from analysis as this indicates potential degassing caused by

173   disturbance during chamber placement. This resulted in loss of 24% of the data.

174

175   *Tree biomass and NPP*

176   Within the tree survey plots described above (see study site), diameter at breast height (dbh)

177   was measured for all trees taller than 140 cm (tall trees). The height of trees 140 cm and shorter

178   was measured (short trees). As all but one of the trees encountered were *Picea mariana* (Mill.)

179   BSP, aboveground biomass of tall trees was estimated using an allometric equation for that species

180   according to Grigal and Kernik (1984). Short tree biomass was estimated as a function of height

181   using the equation determined by Munir *et al*. (2014) also for *Picea mariana*. Belowground

182   biomass was estimated from aboveground biomass using the softwood tree equations of Li *et al*.

183   (2003).

184   In order to estimate tree NPP, tree disks were collected in August from breast height for

185   three tall trees at each tree survey plot. One tree was sampled from each of three dbh classes (1–

186   1.5 cm, 1.5–2.5 cm and 2.5–5 cm). In the laboratory, disks were sanded and scanned using an

187   optical scanner. Tree ring widths were measured using DendroScan (Varem-Sanders & Campbell,

188   1996) and 2013 tree rings were used to estimate NPP to ensure a full annual ring width was

189   included. Ring widths were not significantly related to dbh (linear regression, $F_{1,28} = 0.15$, $p = 0.70$,

190   see also Supporting Information, Figure S1), thus aboveground NPP for large trees was estimated

191   by subtracting the mean ring width of the triplicate trees sampled at each location from the dbh of

192   all trees within that plot, recalculating the biomass and determining the difference (Szumigalski &

193   Bayley, 1996). For small trees, the leader length (annual apical growth) was measured during the

194   tree survey. This was subtracted from the height, and previous year biomass estimated and the

195   difference calculated as aboveground NPP. In both cases, belowground NPP was estimated as the

196   difference in belowground biomass estimated from the Li *et al*. (2003) equation based on the

197   relative aboveground biomass in each year. Biomass estimates were converted to C assuming

198   biomass C content of 50%.

199

200   *Environmental variables*

201   Near surface (top 10 cm) peat samples were collected along three transects (Figure 1) in

202   July 2015 by hand cutting with a serrated knife. Samples were frozen in the laboratory and re-

203   sampled when frozen to obtain an accurate volume (~10×10×10 cm). Peat was dried at 70 °C for

204   120 hours and weighed to determine bulk density.

205   During each C flux measurement, water table was measured relative to the peat surface in

206   a standpipe installed adjacent to each sampling plot. Temperature profiles in 5 cm intervals to a

207   depth of 30 cm were measured using a thermocouple thermometer. If ice was encountered in the

208   top 30 cm during soil temperature measurement, the depth of the frost table was recorded. In

209   August, vegetation cover was estimated in each sampling plot. Cover of functional groups (moss,

210   forb, graminoid, shrub, tree) was estimated to the nearest 1%.

211   Air temperature was measured continuously at a meteorological station location ~200 m

212   from the study site. This was regressed against the soil temperature measurements at each plot to

213   construct a continuous soil temperature record. Solar radiation was measured at the weather station

214   (EM50 with PYR sensor, Decagon Devices Inc. Washington, USA) and converted to

215   photosynthetically active radiation (PAR) based on a regression of solar radiation and PAR

216   measurements made at the time of C flux sampling with a sensor connect to the IRGA.

217

218   *Data analysis*

219   All statistical analyses were completed in R (R Core Team, 2013). Differences between

220   understory C fluxes and environmental conditions between sides of the road and distance from the

221   road were estimated using a linear mixed effects model (package nlme, Pinheiro *et al*., 2014) where

222   plot was included as a random factor to account for repeated measures, and plots on the road were

223   assigned a unique category. If significant differences occurred ($p < 0.05$), pairwise comparison

224   with Tukey correction was applied to evaluate differences between each group (package multcomp,

225   Hothorn *et al*., 2008). Controls on spatial variation in mean study period understory C fluxes were

226   evaluated using linear regression. We investigated the effect of vascular plant cover (and graminoid

227   cover for CH_4), moss cover, water table position and soil temperature. Initially all independent

228   variables and two-way interactions were included. Non-significant factors were then eliminated

229   starting with the least significant and statistical values reported are from models that contained only

230   significant variables. In all cases, seasonal mean values were used in the analysis. Methane flux

231   was log transformed ($\log_{10}(CH_4$ flux $+ 5)$) prior to analysis. Following this transformation, all C

232   flux components were normally distributed (Shapiro-Wilks, $p > 0.05$).

233   Growing season CO_2 exchange in the understory was estimated by modeling GEP and ER

234   for each sample plot. Gross ecosystem photosynthesis was related to PAR using a rectangular

235   hyperbola:

$$GEP = \frac{PAR \, \acute{} \, Q \, \acute{} \, GP_{max}}{(PAR \, \acute{} \, Q + GP_{max})}$$

236   (1)

237   where Q is the quantum efficiency and describes the initial slope of the hyperbola and GP_{max} is the

238   theoretical maximum rate of GEP and represents the asymptote of the hyperbola. Equation 1 was

239   fit separately at each plot using the combined data set from 2014 and 2015 with separate equations

240   generated for May (early season) and June-September (growing season). For plots on the winter

241   road, a large shift occurred in September fluxes and thus growing season included only June –

242   August data with a separate equation fitted to September data.

243   Ecosystem respiration was modelled according to Lloyd and Taylor (1994) related to soil

244   temperature at 5 cm (T5):

$$ER = ER_{ref} \times e^{E0\left[\frac{1}{Tref-T0} - \frac{1}{T5-T0}\right]}$$

245   (2)

246 where ER_{ref} is ER at the reference temperature (Tref = 283.5K), E0 is the activation energy, T0 is

247 the temperature at which biological processes start (237.48K). Both GEP and ER models were fit

248 using Solver in Excel by minimizing the sum of squares error. Error in modelled understory net

249 CO_2 exchange ($E_{NEus-mod}$) at each plot was estimated according to Adkinson $et\ al.$ (2011) by

250 comparing the NE_{us} estimated by the sum of the modelled GEP and ER for the given sampling day

251 (NE_{us-mod}) to the measured NE_{us} (NE_{us-obs}) on that day according to:

252 $$E_{NEus-mod} = \sqrt{\sum_{i=1}^{n} \frac{(NE_{us-obs} - NE_{us-mod})^2}{(n-1) \times n}} \qquad (3)$$

253 Seasonal net CO_2 exchange of the understory (NE_{us}) was estimated over a 153-day study period

254 (May 1 to September 30) using environmental conditions measured at the meteorological station

255 in 2015 combined with equations 1 and 2 and parameters determined for each sampling plot.

256   Mean daily CH_4 flux was used to estimate understory growing season CH_4 flux by

257 multiplying the mean by the number of days in the study period (153 days) as no significant

258 relationship between instantaneous CH_4 flux and T5 or WT was observed. Values were converted

259 to annual fluxes by adding 15% to ER and CH_4 to account for the non-growing season (Saarnio et

260 al., 2007). While this adjustment likely adds substantial uncertainty to annual estimates, it has been

261 used in the Wetland Supplement (IPCC, 2014) to convert growing season peatland fluxes to annual

262 fluxes thereby enabling estimation of annual GHG emission estimates that are needed for national

263 inventory reporting. In future, measurements of wintertime fluxes should be included to reduce

264 uncertainty in annual emission estimates.

265   Ecosystem C balance (NEE) was estimated according to:

266      $$NEE = NE_{us} + NPP_{tree\_ag} + NPP_{tree\_bg} + L_{tree} - Rr + CH_{4us}, \qquad (4)$$

267 where NE_{us} represents annual net exchange of CO_2 in the understory (g C m^{-2}), NPP_{tree_ag} and

268 NPP_{tree_bg} represent annual aboveground and belowground tree C uptake, respectively, L_{tree}

269   represent annual tree litterfall, Rr represents tree root respiration and CH_{4us} represents the annual

270   understory CH_4 flux (modified from Munir *et al.*, 2014) with all flux components expressed in g C

271   m^{-2}. We did not measure L_{tree} or Rr in this study. We estimated L_{tree} as 17% of aboveground tree

272   NPP based on measurements from Szumigalski and Bayley (1996). Estimates of Rr were based on

273   the relationship between measured Rr and tree NPP (Rr = 0.639(NPP) + 17.189), constructed from

274   data presented in Munir *et al.* (2015) and applied to our measured tree NPP data.

275

276   **Results**

277   *Environmental conditions*

278   Long-term mean May to September temperature and precipitation (1981 – 2010) measured

279   approximately 40 km from the study site at the Peace River airport (station: Peace River A) was

280   13.0 °C and 255 mm, respectively. During the same period in 2014 conditions were much warmer

281   and drier with mean temperature of 14.2 °C and precipitation of 124 mm, less than half of the long-

282   term average. Conditions in 2015 were close to the long-term mean with mean temperature of 13.5

283   °C   and   precipitation   of   251   mm.   All   climate   data   is   available   at

284   http://climate.weather.gc.ca/historical_data/search_historic_data_e.html.

285   In general, significant differences in plant cover, soil temperature, bulk density and water

286   table position were found between the winter road and the surrounding peatland, but not among

287   the different sites within the peatland (Table 1). The winter road had significantly greater graminoid

288   cover than the understory of the peatland on either side (north vs. winter road, p < 0.0001; south

289   vs. winter road, p < 0.0001), resulting in significantly greater vascular plant cover on the winter

290   road, although the difference was only significant compared to the north side (p = 0.0007; south

291   vs. winter road, p = 0.06). In this case, the plots on the north side of the winter road had significantly

292 greater vascular plant cover than the south side (p = 0.03). No significant effect of distance from

293 the road was observed for either graminoid or total vascular plant cover and there was no significant

294 interaction between distance and side of the road.

295   Mean soil temperature at 5 cm depth during the study period was greatest on the winter

296 road at 16.4 °C (Table 1). This was significantly higher than the north side of the road (p =

297 0.002), but not the south side of the road (p = 0.80). When measuring soil temperature profiles,

298 we measured the top 30 cm of the peat and recorded when we encountered frozen soil. Based on

299 this data, an estimate of the date of ground thaw in the top 30 cm can be made. In 2015, thaw

300 occurred prior to May 12 on all plots on the winter road, between May 12 and June 10 on the

301 north side, and between May 12 and June 25 on the south side.

302 **Table 1**: Average (standard error)[a] environmental conditions and plant cover at study plots[b]

Location	Water table (cm)[c]	5 cm soil temperature (C)	Bulk density (g cm^{-3})	Moss cover (%)	Total vascular plant cover (%)	Graminoid cover (%)	Shrub cover (%)
Winter road	-6.9 a (1.5)	16.4 a (0.7)	0.16 a (0.02)	20 a (9)	55 (8) a	53 (6) a	0 (0)
North 1m	-14.4 ab (1.4)	16.3 a (0.7)	0.11 ab (0.003)	54 b (12)	33 (4) b	3 (2) b	15 (5)
North 5m	-13.0 ab (1.7)	13.3 ab (0.7)	0.08 b (0.02)	59 b (11)	38 (4) ab	2 (2) b	17 (3)
North 10m	-18.6 b (1.6)	12.9 b (0.8)	0.10 ab (0.02)	66 b (8)	34 (8) b	1 (1) b	15 (13)
South 1m	-7.6 a (1.6)	12.0 b (0.9)	0.06 b (0.009)	47 ab (6)	46 (5) ab	1 (1) b	15 (10)
South 5m	-9.0 a (1.5)	12.2 b (0.8)	0.07 b (0.01)	46 ab (18)	45 (2) ab	3 (2) b	25 (21)
South 10m	-8.9 a (1.7)	11.4 b (1.0)	0.04 b (0.004)	56 b (12)	40 (11) ab	5 (4) b	13 (6)

303 a. Each water table value is average of three plots over the study period (June 1 to September 29). Vegetation cover
304 was estimated visually in late August. Three plots were present at each location.
305 b. values are statistically significantly different from each other at the p=0.05 level if they share no letters in
306 common.

307 c. negative values indicate depth below the peat surface

308

309 Bulk density was highest on the winter road, but was only significantly different than plots

310 on the south side of the road (Table 1). Absolute water table elevation indicated a hydraulic gradient

311 from south to north, but no obvious backup of water adjacent to the winter road (data not shown).

312 Water table relative to the peat surface was significantly shallower on the winter road. The

313 difference was only significant compared to the north side ($p = 0.0012$) while the south side was

314 also significantly wetter than the north ($p = 0.0012$), but not different from the winter road ($p =$

315 0.25). Distance from the road had no significant effect on water table and there was no interaction

316 between distance and side of the road.

317

318 *Understory carbon fluxes*

319 As with environmental conditions, differences between the understory CO_2 and CH_4 fluxes

320 were greatest between the winter road and the surrounding peatland, with few significant effects

321 of distance from the winter road (Table 2). Both GEP_{max} and $NEus_{max}$ indicated significantly greater

322 CO_2 uptake on the winter road than in the understory of the neighbouring peatland. The difference

323 in ER was limited, with only a weak significant difference between the north side and the winter

324 road ($p = 0.049$). Methane flux was high on the winter road (Table 2) and significantly greater than

325 the surrounding peatland (winter road vs. north, $p = 0.01$; winter road vs. south, $p < 0.001$). The

326 north side also had significantly higher understory CH_4 flux than the south side ($p = 0.003$).

327 Variation in understory CO_2 and CH_4 fluxes were correlated to ecohydrological conditions

328 at the study plots (Figures 2 and 3). Total vascular plant cover was a strong predictor for GEP_{max}

329 (linear regression, $R^2=0.54$, $F_{1,18} = 16.0$, $p = 0.0008$) and $NEus_{max}$ ($R^2= 0.50$, $F_{1,18} = 12.2$, $p =$

330 0.003). Water table was also significantly related to $NEus_{max}$ ($R^2=0.43$, $F_{1,19} = 14.3$, $p = 0.001$) and

331 ER ($R^2 = 0.39$, $F_{1,19} = 12.2$, $p = 0.002$). Ecosystem respiration was also related to tree NPP ($F_{1,19} =$

15

332 9.1, p = 0.007). Water table was not significantly related to log(CH_4 flux) ($F_{1,19}$ = 0.3, p = 0.58),

333 but log(CH_4) was significantly positively related to T5 (R^2 = 0.55, $F_{1,19}$ = 23.3, p < 0.001).

334 Graminoid cover was also significant for explaining variation in log(CH_4 flux) (R^2 = 0.53, $F_{1,19}$ =

335 21.1, p = 0.0002); however, this was largely driven by difference in graminoid cover between the

336 undisturbed peatland and the winter road and there is no significant relationship if these points on

337 the winter road are removed (Figure 3b).

338 **Table 2:** Average (standard error)[a] understory CO_2 and CH_4 fluxes at sample plots

Location	GEPmax[b] (g CO$_2$ m^{-2} d^{-1})	ER[c] (g CO$_2$ m^{-2} d^{-1})	NEus-max[b] (g CO$_2$ m^{-2} d^{-1})	CH$_4$ flux (mg CH$_4$ m^{-2} d^{-1})
Winter road	-33.8 (4.7) a	12.7 (2.7)	-20.5 (1.0) a	479 (138) c
North 1m	-17.3 (5.3) b	22.1 (2.0)	5.5 (5.0) bc	93 (26) c
North 5m	-10.9 (1.6) b	18.1 (2.0)	10.9 (2.5) cd	57 (25) bc
North 10m	-8.9 (2.0) b	19.8 (2.0)	18.3 (3.1) d	4.9 (1.2) ab
South 1m	-17.0 (2.9) b	17.4 (0.5)	1.0 (2.7) bc	5.0 (3.0) a
South 5m	-17.7 (1.7) b	16.5 (3.3)	-0.9 (4.6) bc	16 (13) ab
South 10m	-14.7 (1.0) b	10.7 (2.9)	-3.8 (0.7) b	6.3 (2.4) a

339 a. All values are the average of three plots over measured over the study period May – September 2014 and
340 2015. Locations are significantly different from each other if they share no letters in common. There were
341 no significant differences between locations for ER.
342 b. GEPmax is gross ecosystem photosynthesis and NEusmax is net ecosystem exchange of CO_2 in the
343 understory both measured under full light conditions.
344 c. ER is ecosystem respiration, measured in the dark.
345
346 *Tree biomass and NPP*

347   Tree stand density was 1700–26700 stems ha^{-1} with dbh across all study plots of 0.8–10.2

348 cm with a mean of 2.6 cm. Additional details about number of annual growth rings in trees sampled

349 and tree ring widths are given in Supporting Information, Table S1. Trees were removed from the

350 winter road and thus there was no tree biomass and tree NPP was eliminated. Total tree biomass

351 was significantly higher on the north side of the road than the south side, but there was no difference

352 related to distance from the road (Table 3; ANOVA, side – $F_{1,12}$ = 15.2, p = 0.002; distance – $F_{2,12}$

353 = 0.025, p = 0.97). Similarly, NPP was significantly higher on the north side than the south

354 (ANOVA, $F_{1,12}$ = 5.4, p = 0.04). In contrast, there were no significant differences in tree ring widths

16

355   between the sides of the road ($F_{1,30} = 0.45$, p = 0.50) or with distance from the road ($F_{2,30} = 0.91$, p

356   = 0.41) and no interaction between the two ($F_{2,32} = 0.34$, p = 0.71). Average tree ring width was

357   0.31 mm.

358

359   *Estimated carbon balance*

360   Since differences in understory C fluxes and tree biomass were generally only significant

361   between the winter road and the undisturbed peatland and occasionally dependent on the side of

362   the road, annual C flux estimates were summarized by side of the road without considering distance

363   from the winter road (Table 4). Models generally fit the data well with estimated error in growing

364   season NE_{us} varying between 22 and 66 g C m^{-2} (see Supporting Information for parameters and

365   error estimates, Table S2). Understory GEP was on average (standard deviation) -620 (82), -272

366   (87) and -332 (94) g C m^{-2} on the winter road, to the north, and to the south of the road, respectively.

367   Average understory ER during the study period was 432 (175), 538 (91), 507 (125) g C m^{-2}, with

368   annual values (corrected by adding 15% for non-growing season) of 497 (201), 618 (105) and 582

369   (144) g C m^{-2} on, north and south of the road, respectively. Using study period GEP and annual ER

370   estimates resulted in annual NE_{us} of -123 (121), 345 (127) and 247 (96) g C m^{-2} at the same

371   locations, where positive values indicate a source to the atmosphere. Once tree NPP, litterfall, root

372   respiration and CH_4 fluxes were considered, estimated annual C balance on the winter road was -

373   79 (128) g C m^{-2} compared to 161 (163) g C m^{-2} north of the road and 129 (141) g C m^{-2} south of

374   the road.

375
376

Table 3: Estimated mean (standard deviation) tree biomass and net primary productivity (NPP) at distances relative to the winter road

	Tree biomass (g C m^{-2})			NPP (g C m^{-2} yr^{-1})		
	Above-ground	*Below-ground*	*Total*	*Above-ground*	*Below-ground*	*Total*
Winter road	0	0	0	0	0	0
North 1m	1970 (1050)	440 (230)	2410 (1290)	66 (27)	15 (6)	81 (33)
North 5m	2210 (510)	490 (110)	2710 (630)	65 (4)	14 (1)	79 (5)
North 10m	1560 (420)	350 (90)	1910 (510)	58 (13)	13 (3)	71 (16)
South 1m	750 (640)	170 (140)	920 (780)	48 (18)	11 (4)	59 (23)
South 5m	470 (130)	100 (30)	580 (160)	26 (12)	6 (3)	32 (14)
South 10m	1000 (690)	220 (150)	1230 (840)	54 (24)	12 (5)	66 (29)

Table 4: Estimated carbon balance (NEE) and its components[a]

g C m^{-2} yr^{-1}	Winter Road	North Side	South Side
NE_{us}[b]	-144 (119)	349 (143)	244 (87)
NPP_{tree_ag} + NPP_{tree_bg}	0	-85 (21)	-46 (21)
L_{tree}[c]	0	-14 (4)	-9 (4)
Rr[d]	0	81 (13)	54 (14)
CH_{4us}[e]	56 (42)	5 (7)	1 (0.8)
NECB	**-79 (128)**	**161 (163)**	**129 (141)**

a. See equation 3 for definition of all C exchange components. All values are mean (standard deviation). Samples sizes are: winter road – n=3, north side – n=6, south side – n=6. Positive values indicate loss of C from the ecosystem to the atmosphere.
b. estimated based on equation 1 and 2 for the growing season (June 1 to August 31). Ecosystem respiration was increased by 15% to estimate annual values.
c. estimated as 17% of aboveground tree NPP
d. estimated from total tree NPP based on data from Munir et al. (2015)
e. estimated as mean from growing season measurements with an additional 15% added to estimate annual total

Discussion

The construction and use of a winter road through a treed fen in boreal Alberta altered ecohydrological conditions on the winter road resulting in changes to CO_2 and CH_4 fluxes; however, there is little evidence of direct impact on the adjacent peatland. Trees were removed for creation of the winter road and it is unlikely they will recolonize the site in the short term due to shallow water table position (Wieder & House, 2012; Caners & Lieffers, 2014; van Rensen *et al.*, 2015). The wet conditions likely arose due to compression of the peat under the winter road by

398   movement of heavy machinery along this corridor, resulting in the higher bulk density observed.

399   Williams *et al.* (2013) report subsidence of linear disturbances in permafrost peatland due to

400   increasing active layer thickness. Similarly, changes in thermal regime may also play a role in the

401   present study as the peat under the winter road thawed earlier than the surrounding peatland. It has

402   also been suggested that the reduction in transpiration due to the removal of trees contributes to the

403   wetter conditions (Vitt *et al.,* 1999). The changes in tree canopy cover and wetter conditions on the

404   winter road were also likely the drivers of the observed shift in ground layer vegetation to one

405   largely dominated by graminoids. Further ecological studies are needed to further investigate

406   vegetation community changes on winter roads through peatlands.

407   Both CO_2 and CH_4 understory fluxes were significantly different on the winter road

408   compared to the adjacent peatland. Since water table, soil temperature and plant cover were

409   significant factors in explaining variability in ground layer fluxes (Figures 2 and 3), the

410   ecohydrological changes that occurred on the winter road were likely the drivers of the altered C

411   flux. In the study year, we estimated that the undisturbed peatland was an annual source of C to the

412   atmosphere while the winter road was a sink. There was large variability between plots in the

413   undisturbed peatland (Table 4) with some acting as small sinks and others as large sources. The

414   loss of C from the undisturbed peatland may be linked to the dry conditions during the study period,

415   specifically in 2014, as has been reported in other peatland studies (e.g., Alm *et al*., 1999, Strack

416   & Zuback 2013). There is also relatively large uncertainty in the C balance estimated at any given

417   plot due to fact that tree NPP was measured at a different scale than soil C flux and that litter

418   production and tree root respiration were estimated based on literature values. Even considering

419   these uncertainties, the winter road is likely accumulating C at a faster rate than the adjacent

420   peatland suggesting that its elevation will rise over time, resulting in a deeper water table similar

421   to pre-disturbance conditions. The timescale for this transition is unknown, but seismic lines

422   through fens have been observed to persist on the landscape for up to 50 years (van Rensen *et al.*,

423   2015) indicating that recovery is a slow process.

424   Probably the most substantial change was the large increase in CH_4 flux on the winter road

425   (Table 2) that largely appeared linked to warmer soil conditions and the greater cover of graminoids

426   compared to the adjacent peatland (Figure 3). Although many studies have found water table to be

427   the most important factor explaining spatial variation in peatland CH_4 flux (Couwenberg & Fritz,

428   2011; Strack *et al.*, 2016), it was not a significant predictor in the present study. However, the

429   wetter conditions on the road have likely contributed to the shift towards a graminoid-dominated

430   plant community, and also the warmer soil temperature. This corresponds to earlier findings that

431   the strong vegetation control on peatland C flux is species-specific and different plant

432   groups/vegetation classes/species composition can be used for estimating peatland CH_4 emissions

433   after land-use change and/or restoration (Joabsson & Christensen, 2001, Ström *et al.*, 2005, Dias

434   *et al.*, 2010). In our study, the change from tree-shrub-moss-dominated communities of the

435   surrounding peatlands to the graminoid-dominated open community on the winter road can be used

436   to predict increased CH_4 emission.

437   In permafrost regions, wetter conditions on cutlines increase thermal conductivity, resulting

438   in permafrost thaw (Williams & Quinton, 2013). Plots on the winter road were thawed by early

439   May in both 2014 and 2015 while some plots in the adjacent peatland remained frozen until late

440   June. This resulted in warmer soil conditions (Table 1) allowing greater microbial activity and

441   ultimately CH_4 production in the saturated soil conditions. Despite enhanced CO_2 uptake, the

442   substantial increase in CH_4 flux on the winter road results in enhanced radiative forcing related to

443   GHG exchange in the peatland. The global warming potential (GWP) over a 100-year time frame

444   based on measured CO_2 and CH_4 exchange (where the GWP of CH_4 is 28 times that of CO_2 [Myhre

445   *et al*. 2013]) was on average 2100 g CO_2-e m^{-2} yr^{-1} for the winter road and ~250 and 70 g CO_2-e

446   m^{-2} yr^{-1} north and south of the road in the undisturbed peatland. Lee and Boutin (2006) provide

447   what they call a conservative estimate of 1.5 km per km^2 for density of wide seismic lines (many

448   of which are converted to access paths such as winter roads) in northeastern Alberta. Applying this

449   density to the whole province and assuming that these lines are on average 7 m wide and that

450   peatland cover in Alberta is 103,000 km^2 (Environment and Parks, 2017), results in an estimate of

451   close to 1100 km^2 of peatland area impacted by seismic lines/winter roads. Considering an increase

452   in GWP of ~1900 g CO_2-e m^{-2} yr^{-1} on the line compared to the undisturbed peatland leads to an

453   estimate of ~2 Mt CO_2-e m^{-2} yr^{-1} resulting from these disturbances. While the actual impact of

454   individual cutlines is likely to vary depending on many factors including their orientation, width,

455   age, extent of peat compression, and peatland type (e.g., van Rensen *et al*., 2015), clearly these

456   disturbances could represent a substantial additional source of anthropogenic GHG emissions that

457   is not currently accounted for. Narrower 3-D seismic lines (also called low-impact seismic lines)

458   are also widespread in the region (Dabros *et al*., 2017) and further research is needed to determine

459   what impact these may have on peatland GHG fluxes.

460   Dissolved organic carbon (DOC) export was not considered in this study, but can account

461   for a substantial portion of peatland C balances (e.g., Billett *et al.,* 2004). Although linear

462   disturbances could act as flowpaths that hydrologically connect the landscape and enhance

463   hydrologic export of DOC, heterogeneity of the surface elevation along the disturbance creates

464   depression storage and tends to limit hydrologic connectivity to only the wettest times of year

465   (Williams *et al*., 2013). Nevertheless, future studies should include DOC export estimates both

466   along the winter road and from the neighbouring peatland to better understand potential hydrologic

467   perturbation and its impact on peatland DOC export.

468   Finally, no significant differences in understory C fluxes were observed with distance from

469   the winter road, nor were interactions between side of the road and distance observed. Similarly,

470   although tree biomass and NPP were different between the sides of the disturbance, they did not

471   vary with distance from the cutline, and tree ring widths were not significantly different in space.

472   Therefore, differences in the tree canopy may have resulted from inherent differences in space prior

473   to winter road construction. This suggests that the winter road had little impact on the surrounding

474   peatland at this site, in contrast evidence of edge effects from linear disturbance impacts on boreal

475   upland ecosystems (Dabros *et al.*, 2017). The large amount of spatial variability in CO_2 and CH_4

476   flux between sampling plots due to differences in ecological and edaphic controls in space likely

477   limited the ability of our study to detect edge effects related to the winter road. In order to

478   investigate this in the future, a larger number of replicate sample plots would be required; however,

479   this becomes materially difficult when attempting to measure at a variety of distances from the

480   road on both sides of the disturbance. Moreover, it is difficult to measure ecosystem C balance in

481   a forested peatland using chambers as these ground level measurements also include tree root

482   respiration (Rr) that likely varies greatly in space in relation to location of specific roots and local

483   tree productivity. Although we estimated Rr based on previous literature, this is unlikely to

484   accurately reflect the actual Rr at any specific plot, adding substantial uncertainty to C balance

485   measurements. Finally, estimating annual C balance by adding 15% to growing season estimates

486   leads to additional uncertainty, particularly as disturbance may alter the contribution of non-

487   growing season fluxes to the annual total. Ideally, the impact of winter roads, and other cutlines in

488   peatlands, would be measured at an ecosystem to landscape scale using eddy covariance towers

489   above the tree canopy and comparing fluxes of CO_2 and CH_4 to adjacent undisturbed areas. In

490   practice, cutlines are so prevalent in northern Alberta that finding a peatland area without cutlines

491   nearby to a disturbed area would be difficult, if not impossible. In addition, data prior to the

492   construction of the disturbance would provide valuable baseline information against which any

493   post-construction changes could be compared. Again, this may be difficult in practice as

494   construction plans are often in a state of flux making it difficult to plan in advance the appropriate

495   location to collect pre-disturbance data. Large inter-annual variability in peatland C fluxes (e.g.

496   Roulet *et al*., 2007; Saarnio *et al*., 2007) further complicates this approach, as several years both

497   pre- and post-disturbance would be required to separate disturbance effects from changes resulting

498   from weather differences between the study years. Moreover, the time over which impacts will

499   occur post-disturbance is unknown.

500   In conclusion, construction and use of a winter road through a wooded fen near Peace River,

501   AB, Canada has resulted in warmer and wetter conditions on the winter road and a shift to an open

502   peatland dominated by graminoids. While tree biomass and tree NPP have been removed from the

503   footprint of the winter road, the C balance of the site indicated an enhanced sink compared to the

504   adjacent peatland. On the other hand, CH_4 flux has increased dramatically on the winter road in

505   response to the changing ecohydrological conditions. If this pattern is representative of all wide

506   seismic lines and winter roads through peatlands, then these disturbances will represent an

507   important anthropogenic GHG source associated with land-use. As the magnitude of enhanced

508   GHG flux on cutlines is likely to depend on peatland type and disturbance characteristics (width,

509   traffic and compaction, etc.), more data is needed on a variety of cutlines to better constrain the

510   regional effect. No clear impacts on the C fluxes in the neighbouring peatland were detected, at

511   least in part due to spatial variability in these fluxes and the lack of pre-disturbance data. Therefore,

512 flux measurements pre-disturbance and several years post-disturbance are required to better

513 constrain potential edge effects.

514

515 **Acknowledgements**

521

522 **References**

523 Adkinson, A., Syed, K. H., & Flanagan, L. B. (2011). Contrasting responses of growing season

524   ecosystem CO_2 exchange to variation in temperature and water table depth in two

525   peatlands in northern Alberta, Canada. *Journal of Geophysical Research*, 116, G01004.

526   doi: 10.1029/2010JG001512

527 Alm, J., Schulman, L., Walden, J., Nykänen, H., Martikaninen, P. J. & Silvola, J. (1999). Carbon

528   balance of a boreal bog during a year with an exceptionally dry summer, *Ecology*, 80,

529   161-174.

530 Billett, M. F., Palmer, S. M., Hope, D., Deacon, C., Storeton-West, R., Hargreaves, K. J.,

531   Flechard, C. & Fowler, D. (2004). Linking land-atmosphere-stream carbon fluxes in a

532   lowland peatland system. *Global Biogeochemical Cycles*, 18, GB1024. doi:

533   10.1029/2003GB002058

534 Braverman, M. & Quinton, W.L. (2016). Hydrological impacts of seismic lines in the wetland-

535   dominated zone of thawing, discontinuous permafrost, Northwest Territories, Canada.

536   *Hydrological Processes*, 30, 2617-2627. doi: 10.1002/hyp.10695

537 Bridgham, S. D., Cadillo-Quiroz, H., Keller, J. K. & Zhuang, Q. (2013). Methane emissions from

538   wetlands: biogeochemical, microbial, and modeling perspectives from local to global

539   scales. *Global Change Biology*, 19, 1325-1346. doi: 10.1111/gcb.12131

540 Bubier, J., Crill, P., Mosedale, A., Frolking, S. & Linder, E. (2003). Peatland responses to

541   varying interannual moisture conditions as measured by automatic CO_2 chambers. *Global*

542   *Biogeochemical Cycles*, 17, 1066. doi: 10.1029/2002GB001946

543 Campbell, D. & Bergeron, J. (2012). Natural revegetation of winter roads on peatland in the

544   Hudson Bay Lowlands, Canada. *Arctic, Antarctic, and Alpine Research*, 44, 155-163.

545 Campbell, C., Vitt, D. H., Halsey, L. A., Campbell, I. D., Thormann, M. N. & Bayley, S. E.

546   (2000). *Net primary production and standing biomass in northern continental peatlands*,

547   Information Report NOR-X-369, Edmonton, AB, Canada: Canadian Forest Service,

548   Northern Forestry Centre.

549 Caners, R. T. & Lieffers, V. J. (2014). Divergent pathways of successional recovery for in situ oil

550   sands exploration drilling pads on wooded moderate-rich fens in Alberta, Canada.

551   *Restoration Ecology*, 22, 657-667. doi: 10.1111/rec.12123

552 Choi, W.-J., Chang, S. X. & Bhatti, J. S. (2007). Drainage affects tree growth and C and N

553   dynamics in a minerotrophic peatland. *Ecology*, 88, 443-453.

554 Couwenberg, J. & Fritz, C. (2012). Towards developing IPCC methane 'emission factors' for

555   peatlands (organic soils). *Mires and Peat*, 10, Article 3, 1-17. Available: http://www.mires-

556   and-peat.net/

557   Dabros, A., Hammond, H. E. J., Pinzon, J., Pinno, B., Langor, D. (2017). Edge influence of low-

558   impact seismic lines for oil exploration on upland forest vegetation in northern Alberta

559   (Canada). *Forest Ecology and Management*, 400, 278-288.

560   Dias, A. T. C., Hoorens, B., van Logtestijn, R. S. P., Vermaat, J. E. & Aerts, R. (2010). Plant

561   species composition can be used as a proxy to predict methane emissions in peatland

562   ecosystems after land-use change. *Ecosystems*, 13, 526-538. doi: 10.1007/s10021-010-

563   9338-1

564   Environment and Parks (2017). Reclamation Criteria for Wellsites and Associated Facilities for

565   Peatlands, March 2017, Edmonton, Alberta.

566   Frolking, S., Roulet, N. T. (2007). Holocene radiative forcing impact of northern peatland carbon

567   accumulation and methane emissions. *Global Change Biology*, 13, 1079-1088. doi:

568   10.1111/j.1365-2486.2007.01339.x

569   Gillies, C. (2011). Water management techniques for resource roads in wetlands: A state of practice

570   review, Report prepared by FPInnovations for Ducks Unlimited Canada.

571   Grigal, D. F. & Kernik, L. K. (1984). Generality of black spruce biomass estimation equations.

572   *Canadian Journal of Forest Research*, 14, 468-470.

573   Halsey, L. A., Vitt, D. H., Beilman, D., Crow, S., Mehelcic, S. & Wells, R. (2003). *Alberta

574   Inventory Wetland Classification System Version 2.0*, Edmonton, AB, Canada: Alberta

575   Sustainable Resource Development.

576   Hothorn, T., Bretz, F. & Westfall, P. (2008). Simultaneous inference in general parametric models.

577   *Biometrical Journal*, 50, 346-363.

578   House, M., Vitt, D. H. & Wieder, R. K. (2012). Plant community recover on "minimum

579   disturbance" petroleum sites compared to burned sites in bogs of northern Alberta, In D.

580   Vitt & J. Bhatti (Eds.), *Restoration and reclamation of boreal ecosystems: Attaining*

581   *sustainable development* (pp. 202-217). Cambridge, U.K.: Cambridge University Press.

582   IPCC. (2014). T. Hiraishi, T. Krug, K. Tanabe, N. Srivastava, J. Baasansuren, M. Fukuda & T. G.

583   Troxler (Eds.), *2013 Supplement to the 2006 IPCC Guidelines for National Greenhouse*

584   *Gas Inventories: Wetlands*, Switzerland: IPCC.

585   Joabsson, A. & Christensen, T. R. (2001). Methane emissions from wetlands and their relationship

586   with vascular plants: An Arctic example. *Global Change Biology*, 7, 919-932. doi:

587   10.1046/j.1354-1013.2001.00044.x

588   Lee, P. & Boutin, S. (2006). Persistence and developmental transition of wide seismic lines in the

589   western Boreal Plains of Canada. *Journal of Environmental Management*, 78, 240-250.

590   Li, Z., Kurz, W. A., Apps, M. J. & Beukema, S. J. (2003). Belowground biomass dynamics in the

591   Carbon Budget Model of the Canadian Forest Sector: recent improvements and

592   implications for the estimation of NPP and NEP. *Canadian Journal of Forest Research*, 33,

593   126-136. doi: 10.1139/X02-165

594   Lloyd, J. & Taylor, J. (1994). On the temperature dependence of soil respiration. Functional

595   *Ecology*, 8, 315-323.

596   Loisel, J., Yu, Z., Beilman, D. W., Camill, P., Alm, J., Amesbury, M. J., Anderson, D., Andersson,

597   S., Bochicchio, C., Barber, K., Belyea, L. R., Bunbury, J., Chambers, F. M., Charman, D.

598   J., De Vleeschouwer, F., Fialkiewicz-Koziel, B., Finkelstein, S. A., Galka, M., Garneau,

599   M., Hammarlund, D., Hinchcliffe, W., Holmquist, J., Hughes, P., Jones, M. C., Klein, E.

600   S., Kokfelt, U., Korhola, A., Kuhry, P., Lamarre, A., Lamentowicz, M., Large, D., Lavoie,

601   M., MacDonald, G., Magnan, G., Mäkilä, M., Mallon, G., Mathijssen, P., Mauquoy, D.,

602   McCarroll, J., Moore, T. R., Nichols, J., O'Reilly, B., Oksanen, P., Packalen, M., Peteet,

603 D., Richard, P. J. H., Robinson, S., Tiina, R., Rundgren, M., Sannel, A. B. K., Tarnocai, C.,

604 Thom, T., Tuittila, E.-S., Turetsky, M., Väliranta, M., van der Linden, M., van Geel, B.,

605 van Bellen, S., Vitt, D., Zhao, Y., Zhou, W. (2014). A database and synthesis of northern

606 peatland soil properties and Holocene carbon and nitrogen accumulation. *The Holocene*,

607 24, 1028-1042. doi: 10.1177/0959683614538073

608 Moore, T. R., Trofymow, J. A., Siltanen, M., Kozak, L.M. (2008). Litter decomposition and

609 nitrogen and phosphorus dynamics in peatlands and uplands over 12 years in central

610 Canada. *Oecologia*, 157, 317-325,

611 Munir, T. M., Strack, M. (2014). Methane flux influenced by experimental water table drawdown

612 and soil warming in a dry boreal continental bog. *Ecosystems*, 17, 1271-1285. doi:

613 10.1007/s10021-014-9795-z

614 Munir, T. M., Xu, B., Perkins, M. & Strack, M. (2014). Responses of carbon dioxide flux and plant

615 biomass to water table drawdown in a treed peatland in northern Alberta: a climate change

616 perspective. *Biogeosciences*, 11, 807-820. doi: 10.5194/bg-11-807-2014

617 Munir, T. M., Perkins, M., Kaing, E. & Strack, M. (2015). Carbon dioxide flux and net primary

618 production of a boreal treed bog: Responses to warming and water-table-lowering

619 simulations of climate change. *Biogeosciences*, 12, 1091-1111. doi: 10.5194/bg-12-1091-

620 2015

621 Myhre, G., Shindell, D., Bréon, F.-M., Collins, W., Fuglestvedt, J., Huang, J., Koch, D., Lamarque,

622 J.-F., Lee, D., Mendoza, B., Nakajima, T., Robock, A., Stephens, G., Takemura, T. &

623 Zhang, H. (2013). Anthropogenic and natural radiative forcing. In T. G. Stocker, D. Qin,

624 G.-K. Plattner, M. Tignor, S. K. Allen, J. Boschung, A. Nauels, Y. Xia, V. Bex & P. M.

625 Midgley (Eds). *Climate Change 2013: The Physical Science Basis. Contribution of*

626   *Working Group I to the Fifth Assessment Report of the Intergovernmental Panel on Climate*

627   *Change*, Cambridge, U.K.: Cambridge University Press.

628 Pasher, J., Seed, E. & Duffe, J. (2013). Development of boreal ecosystem anthropogenic

629   disturbance layers for Canada based on 2008 to 2010 Landsat imagery. *Canadian Journal*

630   *of Remote Sensing*, 39, 42-58. doi: 10.5589/m13-007

631 Patterson, L. & Cooper, D. J. (2007). The use of hydrological and ecological indicators for the

632   restoration of drainage ditches and water diversions in a mountain fen, Cascade Range,

633   California. *Wetlands*, 27, 290-304.

634 Pinheiro, J., Bates, D., DebRoy, S, Sarkar, D. & R Core Team (2016). Linear and nonlinear mixed

635   effects models, R package version 3.1-128. http://CRAN.R-project.org/package=nlme.

636 R Core Team (2016). R: A language and environment for statistical computing. R Foundation for

637   Statistical Computing, Vienna, Austria. http://www.R-project.org/.

638 Roulet, N. T., Lafleur, P. M., Richard, P. J. H., Moore, T. R., Humphreys, E. R. & Bubier, J. L.

639   (2007). Contemporary carbon balance and late Holocene carbon accumulation in a northern

640   peatland. *Global Change Biology*, 13, 297-411. doi: 10.1111/j.1365-2486.2006.01292.x

641 Saarnio, S., Morero, M., Shurpali, N. J., Tuittila, E.-S., Mäkilä, M. & Alm, J. (2007). Annual CO_2

642   and CH_4 fluxes of pristine boreal mires as a background for the lifecycle analyses of peat

643   energy. *Boreal Environment Research*, 12, 101-113.

644 Schneider, R. & Dyer, S. (2006). Death by a Thousand Cuts: Impacts of in situ oil sands

645   development on Alberta's boreal forest, The Pembina Institute/CPAWS.

646 Strack, M., Cagampan, J., Hassanpour Fard, G., Keith, A. M., Nugent, K., Rankin, T., Robinson,

647   C., Strachan, I. B., Waddington, J. M. & Xu, B. (2016). Controls on plot-scale growing season

648   CO_2 and CH_4 fluxes in restored peatlands: Do they differ from unrestored and natural sites.

649   *Mires and Peat*, 17, Article 5, Available: http://www.mires-and-peat.net/. doi:

650   10.19189/MaP.2015.OMB.216

651   Strack, M., Mwakanyamale, K., Hassanpour Fard, G., Bird, M., Bérubé, V., & Rochefort, L.

652   (2017). Effect of plant functional type on methane dynamics in a restored minerotrophic

653   peatland. *Plant and Soil*, 410, 231-246.

654   Strack, M., Waddington, J. M. & Tuittila, E.-S. (2004). Effect of water table drawdown on northern

655   peatland methane dynamics: Implications for climate change. *Global Biogeochemical Cycles*,

656   18, GB4003, doi: 10.1029/2003GB002209.

657   Strack, M., Waddington, J. M., Rochefort, L. & Tuittila, E.-S. (2006). Response of vegetation and

658   net ecosystem carbon dioxide exchange at different peatland microforms following water table

659   drawdown. *Journal of Geophysical Research*, 111, G02206, doi: 10.1029/2005JG000145.

660   Strack, M. & Zuback, Y. C. A. (2013). Annual carbon balance of a peatland 10 yr following

661   restoration. *Biogeosciences*, 10, 2885-2896. doi: 10.5194/bg-10-2885-2013

662   Ström, L., Mastepanov, M. & Christensen, T. R. (2005). Species-specific effect of vascular plants

663   on carbon turnover and methane emissions from wetlands. *Biogeochemistry*, 75, 65-82. doi:

664   10.1007/s10533-004-6124-1

665   Szumigalski AR & Bayley SE. (1996). Net above-ground primary production along a bog-rich fen

666   gradient in central Alberta, Canada. *Wetlands*, 16, 467-476.

667   Timoney, K. & Lee, P. (2001). Environmental management in resource-rich Alberta, Canada: first

668   world jurisdiction, third world analogue? *Journal of Environmental Management*, 63, 387-

669   405. doi: 10.1006/jema.2001.0487

670   Van Rensen, C. K., Nielsen, S. E., White, B., Vinge, T. & Lieffers, V. J. (2015). Natural

671   regeneration of forest vegetation on legacy seismic lines in boreal habitats in Alberta's oil

672   sands region. *Biological Conservation*, 184, 127-135.

673   Varem-Sanders, T. M. L. & Campbell, I. D. (1996). DendroScan: a tree ring width and density

674   measurement system, Special Report 10, Edmonton, AB, Canada: Canadian Forest Service,

675   Northern Forestry Centre.

676   Vitt, D. H., Halsey, L. A. & Zoltai, S. C. (1999). The changing landscape of Canada's western

677   boreal forest: the current dynamics of permafrost. *Canadian Journal of Forest Research*, 30,

678   283-287.

679   Vitt, D. H., Halsey, L. A., Bauer, I. E. & Campbell, C. (2000). Spatial and temporal trends in carbon

680   storage of peatlands of continental western Canada through the Holocene. *Canadian Journal*

681   *of Earth Sciences*, 37, 683-693.

682   Weltzin, J. F., Bridgham, S. D., Pastor, J., Chen, J. & Harth, C. (2003). Potential effects of warming

683   and drying on peatland plant community composition. *Global Change Biology*, 9, 141-151.

684   Wieder, R. K., Scott, K. D., Kamminga, K., Vile, M. A., Vitt, D. H., Bone, T., Xu, B., Benscoter,

685   B. & Bhatti, J. S. (2009). Postfire C balance in boreal bogs of Alberta, Canada. *Global Change*

686   *Biology*, 15, 63-81. doi: 10.1111/j.1365-2486.2008.01756.x

687   William, T. J. & Quinton, W. L. (2013). Modelling incoming radiation on linear disturbance and

688   its impact on the ground thermal regime in discontinuous permafrost. *Hydrological Processes*,

689   27, 1854-1865. doi: 10.1002/hyp.9792

690   Williams, T.J., Quinton, W. L. & Baltzer, J. L. (2013). Linear disturbances on discontinuous

691   permafrost: implications for thaw-induced changes to land cover and drainage patterns.

692   *Environmental Research Letters*, 8, 025006. doi: 10.1088/1748-9326/8/2/025006.
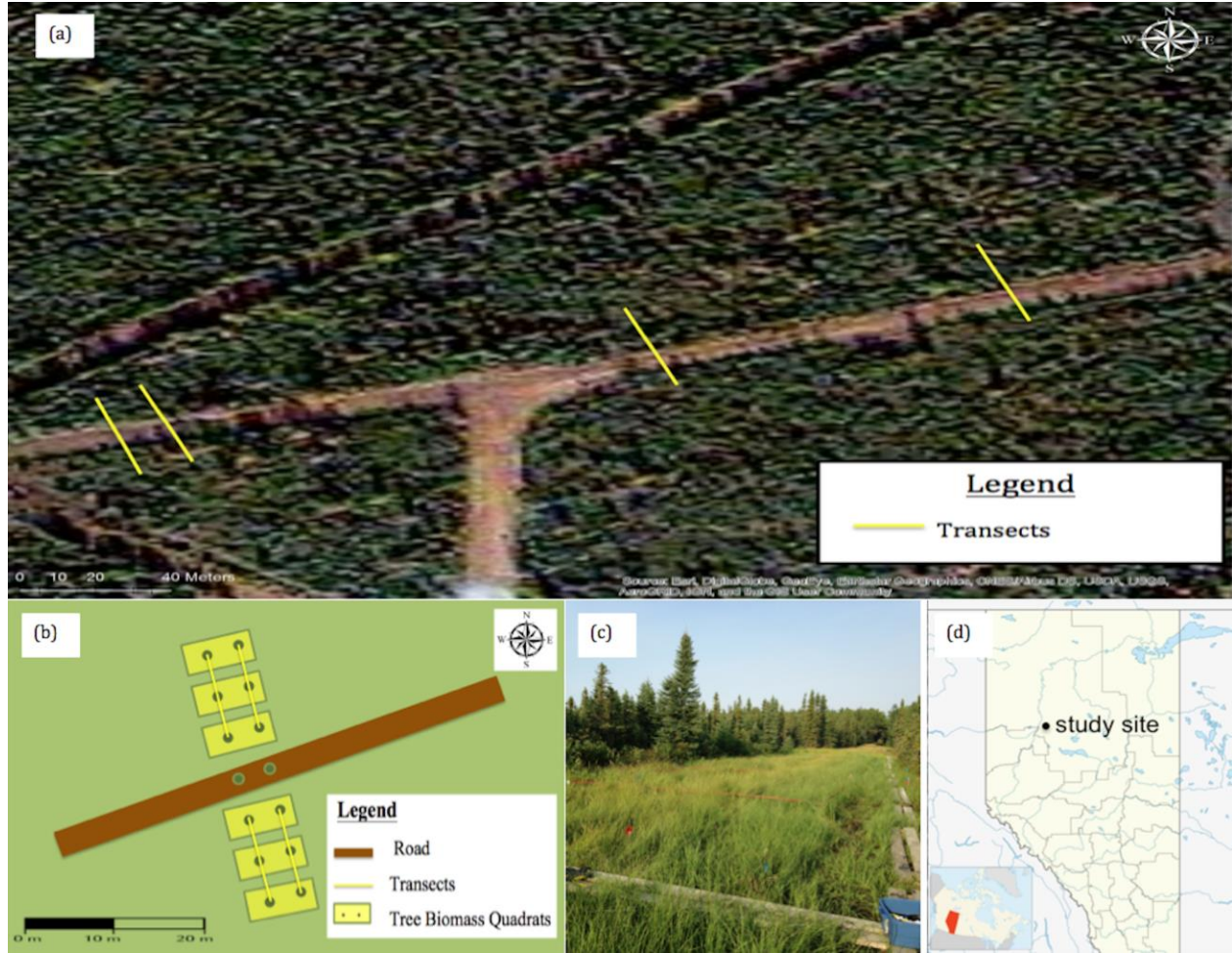
Figures

Figure 1: Study site with transects (a) where C flux measurements were made at two westernmost transects and the eastern transect and bulk density measurements were made between the western transects, and on the middle and eastern transects. (b) Close-up schematic of western transects illustrating C flux measurement plots and trees biomass quadrats. (c) Photograph of winter road with treed peatland on edges. (d) Location of study site within Alberta and Canada (source: http://commons.wikimedia.org/wiki/File:Canada_Alberta_location_map_2.svg#file
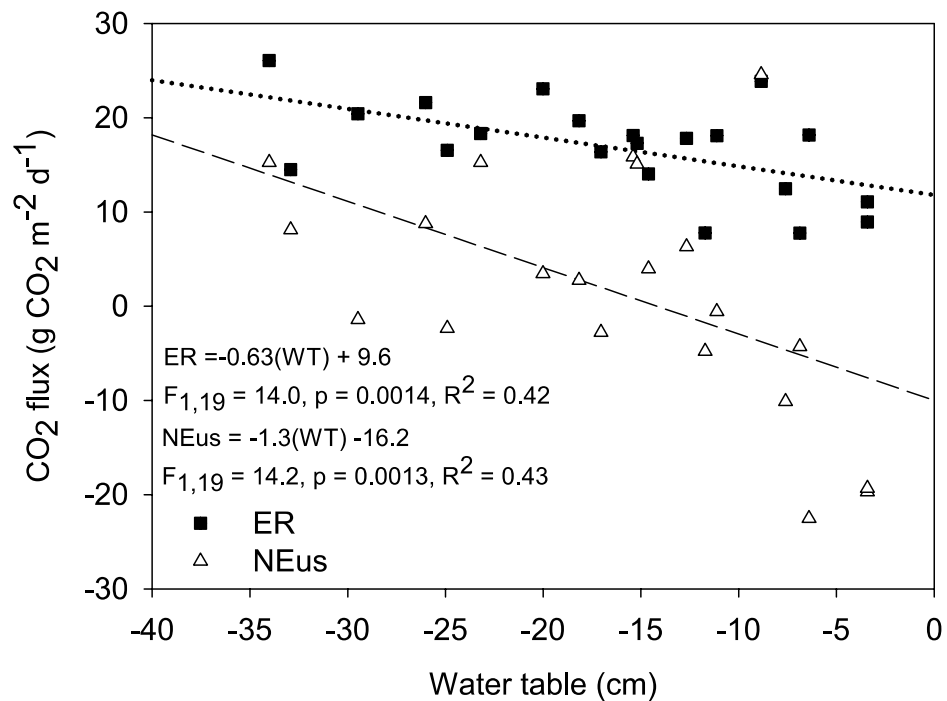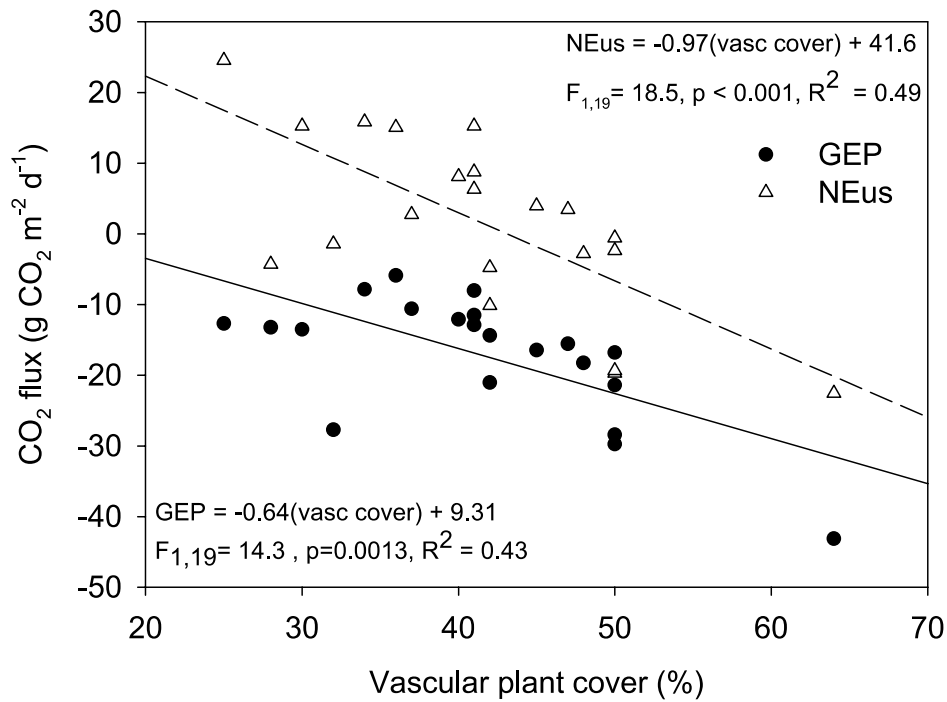
Figure 2: (a) Understory gross ecosystem photosynthesis (GEP) and net ecosystem exchange (NE_{us}) versus vascular plant cover and (b) NE_{us} and ecosystem respiration (ER) versus water table position. All values for GEP and NE_{us} are the mean of all measured fluxes in full light conditions over the study period where positive values indicate release of CO_2 to the atmosphere. Water table position is the mean measured over the study period where negative values indicate depth below the surface.

709
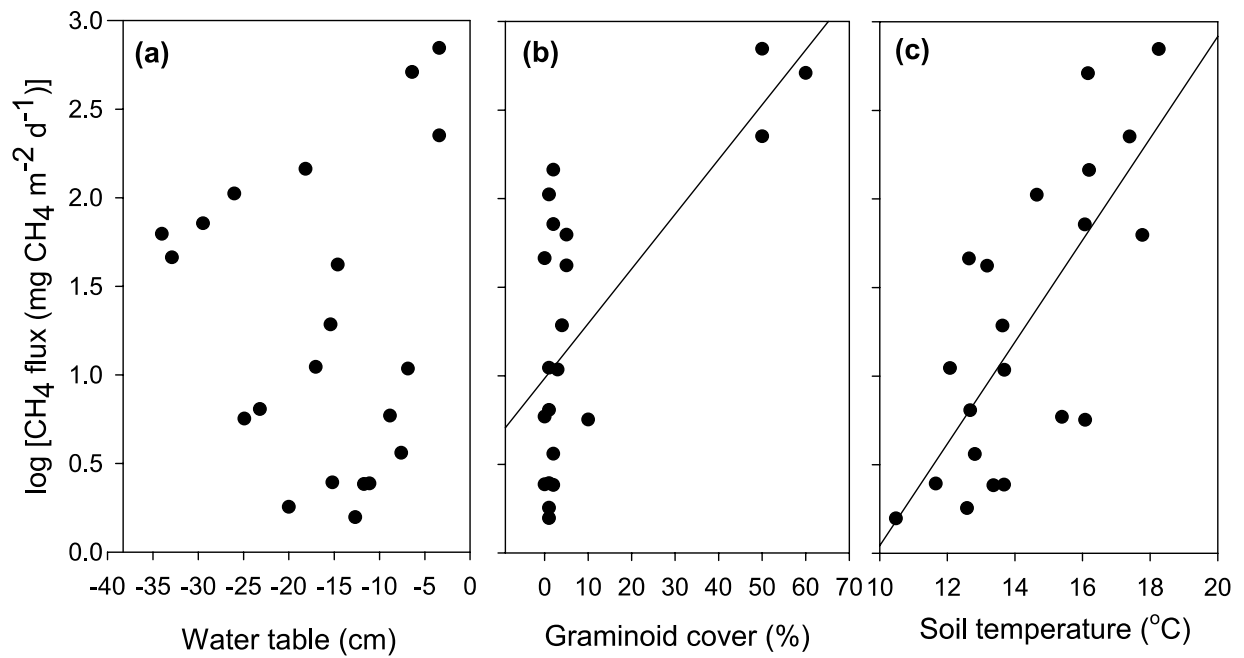
Figure 3: Mean seasonal methane flux (as $\log_{10}$ values) versus (a) water table, (b) graminoid cover and (c) soil temperature at 5 cm depth. All values are means of all measurements over the study period except graminoid cover that was estimated in August 2014. There was no significant relationship between WT and $\log_{10}$(CH4 flux). $\log_{10}$ (CH4 flux) = 0.031(graminoid cover) + 0.98, $F_{1,19}$ = 17.1, p<0.001, R^2 = 0.47; $\log_{10}$(CH4 flux) = 0.29(soil temp) - 2.8, $F_{1,19}$ = 23.3, p<0.001, R^2 = 0.55. Removal of the three points with high graminoid cover from (b) results in no significant relationship for the remaining data set.